Reconfigurable non-blocking four-port optical router based on microring resonators

Lin Yang,* Hao Jia, Yunchou Zhao, and Qiaoshan Chen

State Key Laboratory on Integrated Optoelectronics, Institute of Semiconductors, Chinese Academy of Sciences, P.O. Box 912, Beijing 100083, China

**Corresponding author: oip@semi.ac.cn*

Received January 5, 2015; revised February 6, 2015; accepted February 6, 2015; posted February 9, 2015 (Doc. ID 231925); published March 13, 2015

A reconfigurable non-blocking four-port optical router with the least optical switches is demonstrated. The device is based on microring resonators tuned through thermo-optic effect. The optical signal-to-noise ratio of the device at its nine routing states is about 15 dB. A 25 Gbps data transmission has been performed on its whole 12 optical links, and 8-channel wavelength division multiplexing data transmission has been implemented to expand its communication capacity. The energy efficiency of the device is 23 fJ/bit, and the response time of the device is about 25 μs.

OCIS codes: (200.4650) Optical interconnects; (130.3120) Integrated optics devices; (130.4815) Optical switching devices; (250.5300) Photonic integrated circuits; (230.5750) Resonators.

http://dx.doi.org/10.1364/OL.40.001129

Networks-on-chip (NoCs) for high-performance multi-core processors have attracted substantial interest in recent years [1,2]. However, traditional metallic-interconnect-based NoC gradually becomes a bottleneck for improving the performance of a multi-core processor because of its high power consumption, limited bandwidth, and long latency [3]. Photonic NoC is one alternative interconnection technology that promises high-speed data transmission, low latency, and power consumption [4]. An optical router is an essential component for photonic NoC, which is responsible for switching the data from one optical link to another [5–8].

Several strict non-blocking four-port optical routers based on microring resonators (MRs) have been demonstrated [9–12]. A universal method for constructing a strict non-blocking N-port optical router based on MRs or Mach–Zehnder (MZ) interferometers has also been reported [13,14]. These optical routers have the same characteristic that for a specific input–output optical link in all routing states, the routing path is certain and unique. This characteristic makes their routing algorithms quite simple, while they occupy $N \times (N-2)$ switch elements to establish all possible optical links, where N is the number of port. For example, all reported strict non-blocking four-port optical routers have eight switching elements [9–12]. Reconfigurable non-blocking routing offers the optical router with a prominent characteristic that, for a specific input–output optical link in all routing states, possibly different routing paths can be selected to establish it. An absolutely reconfigurable non-blocking optical router makes full use of the optical links of a 2×2 optical switch and combination of routing paths and, thus, is a hopeful way to compact the structure of optical router. Fewer switch elements mean more efficiency in footprint, power consumption, and latency. A partly reconfigurable non-blocking four-port optical router composed of six switch elements has been reported [15]. In this Letter, a reconfigurable non-blocking four-port optical router with the least MR optical switches is fabricated and characterized. 8×25 Gbps wavelength division multiplexing (WDM) data transmission has been implemented through each optical link of the optical router.

The schematic of the four-port optical router is shown in Fig. 1, where four MRs are used as 2×2 optical switches and four waveguide crossings are included. We denote the optical link from input port i to output port j as $I_i \rightarrow O_j$. A four-port optical router has 12 optical links, among which four optical links including $I_1 \rightarrow O_2$, $I_2 \rightarrow O_1$, $I_3 \rightarrow O_4$, and $I_4 \rightarrow O_3$ can be established passively since the four MR optical switches are off-resonance at the working wavelengths. If the four MR optical switches are removed, the four optical links still can be established. In other words, the four optical links are established with four optical waveguides directly. Thus, there are eight optical links left to be manipulated with on-resonance MR optical switches. Each MR optical switch can, at most, manipulate two optical links simultaneously, so at least four MR optical switches are needed to construct the remaining eight optical links. This is the fewest MR optical switches for a reconfigurable non-blocking four-port optical router.

Table 1 shows the routing table of the four-port optical router. "ON" or "OFF" in the routing table indicate that the corresponding MR optical switch is on- or off-resonance at the working wavelengths. Blocking only occurs when one MR optical switch is on-resonance at the working wavelengths in one optical link while being off-resonance at the working wavelengths in another optical link, while the two optical links should be established simultaneously in a specific routing state.

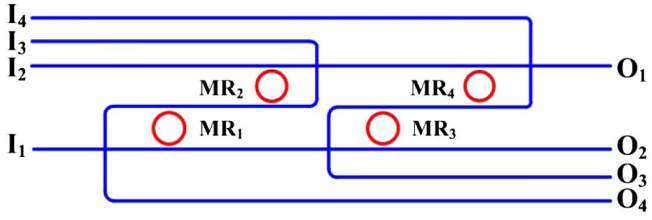

Fig. 1. Schematic of the reconfigurable non-blocking four-port optical router.

Table 1. Routing Tables of Four-Port Optical Router[a]

State	Optical Links	MR1	MR2	MR3	MR4
1	$I_1 \rightarrow O_2$, $I_2 \rightarrow O_1$, $I_3 \rightarrow O_4$, $I_4 \rightarrow O_3$	OFF	OFF	OFF	OFF
2	$I_1 \rightarrow O_4$, $I_2 \rightarrow O_1$, $I_3 \rightarrow O_2$, $I_4 \rightarrow O_3$	ON	OFF	OFF	OFF
3	$I_1 \rightarrow O_2$, $I_2 \rightarrow O_4$, $I_3 \rightarrow O_1$, $I_4 \rightarrow O_3$	OFF	ON	OFF	OFF
4	$I_1 \rightarrow O_3$, $I_2 \rightarrow O_1$, $I_3 \rightarrow O_4$, $I_4 \rightarrow O_2$	OFF	OFF	ON	OFF
5	$I_1 \rightarrow O_2$, $I_2 \rightarrow O_3$, $I_3 \rightarrow O_4$, $I_4 \rightarrow O_1$	OFF	OFF	OFF	ON
6	$I_1 \rightarrow O_4$, $I_2 \rightarrow O_3$, $I_3 \rightarrow O_2$, $I_4 \rightarrow O_1$	ON	OFF	OFF	ON
7	$I_1 \rightarrow O_3$, $I_2 \rightarrow O_4$, $I_3 \rightarrow O_1$, $I_4 \rightarrow O_2$	OFF	ON	ON	OFF
8	$I_1 \rightarrow O_4$, $I_2 \rightarrow O_3$, $I_3 \rightarrow O_1$, $I_4 \rightarrow O_2$	ON	ON	ON	OFF
9	$I_1 \rightarrow O_3$, $I_2 \rightarrow O_4$, $I_3 \rightarrow O_2$, $I_4 \rightarrow O_1$	OFF	ON	ON	ON

[a]ON: on-resonance at the working wavelengths; OFF, off-resonance at the working wavelengths.

From the routing table, blocking does not occur in the nine routing states and, therefore, the optical router is non-blocking.

The device is fabricated on an 8 in. (0.2 m) silicon-on-insulator wafer with a 220 nm thick top silicon layer and a 2 μm thick buried silicon dioxide layer. 180 nm deep ultra-violet photolithography is used to define the pattern, and an inductively coupled plasma etching process is employed to etch the top silicon layer. A rib waveguide with 400 nm in width, 220 nm in height, and 70 nm in slab thickness is employed and the four MRs are covered with titanium nitride micro-heaters to modulate their resonance wavelengths. The micrograph of the device is shown in Fig. 2.

The four MR optical switches are designed with identical physical parameters so that they have same resonance wavelengths. Since the MR optical switch has a periodic filtering spectrum, it can manipulate the WDM optical signals with channel spacing equal to the MR's free spectral range (FSR). Therefore, the aggregate bandwidth of the optical router based on MR optical switches can be expanded through WDM. Principally, increasing the radius of the MR optical switch can increase the aggregate bandwidth while its footprint increases simultaneously. As a trade-off between aggregate bandwidth and footprint, the radii of the MRs are chosen to be 20 μm.

An amplified spontaneous emission source and an optical spectrum analyzer are employed to measure the static spectral response of the device. To characterize the static spectral response of each MR optical switch and determine the working wavelengths, we choose two special optical links, $I_1 \rightarrow O_2$ and $I_2 \rightarrow O_1$, which suitably cover four MR optical switches. Figure 3 shows the transmission spectra of the four MR optical switches in the optical links, $I_1 \rightarrow O_2$ and $I_2 \rightarrow O_1$. The MR with the

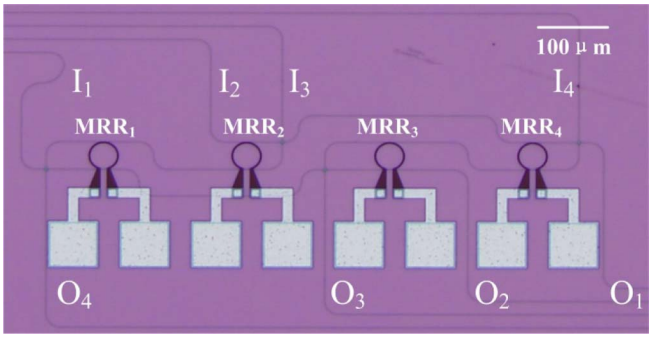

Fig. 2. Micrograph of the fabricated four-port optical router.

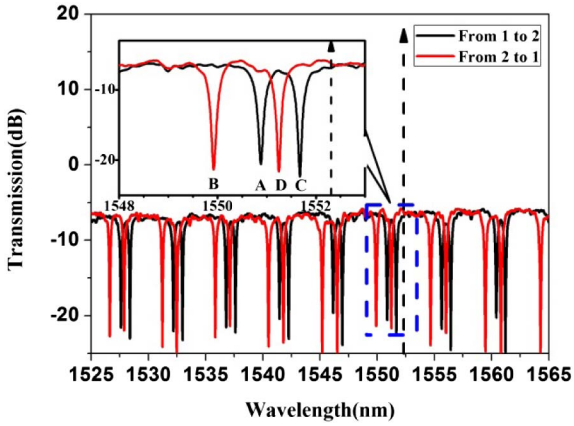

Fig. 3. Response spectra of the four MR optical switches of the device.

radius of 20 μm has a FSR of about 5 nm, which means that, in the wavelength range from 1525 to 1565 nm, it can manipulate eight-wavelength optical signals with the interval equal to the FSR. The inset shows the magnified spectral response of the four MR optical switches near 1550 nm. Four MR optical switches have somewhat different resonance wavelengths because of the inevitable fabrication error, which can be compensated by thermo-optic tuning with extra power consumption. Based on the resonance wavelengths of the four MR optical switches, we choose 1552.31 nm as the working wavelength in the FSR near 1550 nm, which is labeled by the dashed line with arrow. The measured Q factors for the four MRs are 4851, 4566, 5174, and 5007 and the corresponding coupling coefficients are 0.384, 0.428, 0.409, and 0.421.

To characterize the optical crosstalk and signal-to-noise ratio (SNR) of the four-port optical router in all routing states, four tunable voltage sources are employed to adjust four MR states. Figure 4 shows the spectral response of the optical router in its nine routing states. In routing state 1, four MR optical switches are off-resonance at the working wavelengths, and four optical links, $I_1 \rightarrow O_2$, $I_2 \rightarrow O_1$, $I_3 \rightarrow O_4$, and $I_4 \rightarrow O_3$, are established. In Fig. 4(a), the red line shows the spectral response of the optical link $I_2 \rightarrow O_1$ in routing state 1, and the other three lines show the spectral responses of the optical links $I_1 \rightarrow O_1$, $I_3 \rightarrow O_1$, and $I_4 \rightarrow O_1$. Note that these three optical links are not established in routing state 1, and therefore are the noise to the optical link $I_2 \rightarrow O_1$. The SNRs are 13.0–20.1 dB for all 36 optical links of the nine routing states. Relatively low optical SNRs are mainly caused by the relatively low extinction ratios of the MRs. High-order MRs [16,17] can be utilized to improve this performance.

To verify the functionality of the optical router, high-speed data transmissions are implemented for all 12 optical links. An MZ intensity modulator is used to externally modulate the continuous light at the wavelength of 1552.31 nm generated by a tunable laser. 25 Gbps 2^{31} – 1 pseudo-random bit sequence is generated by a pulse pattern generator. The output optical signal is sent to a digital communication analyzer for eye diagram observation. The eye diagrams are shown in Fig. 5. Note that all eye diagrams are taken with a single channel propagating. Clear and open eye diagrams verify the signal

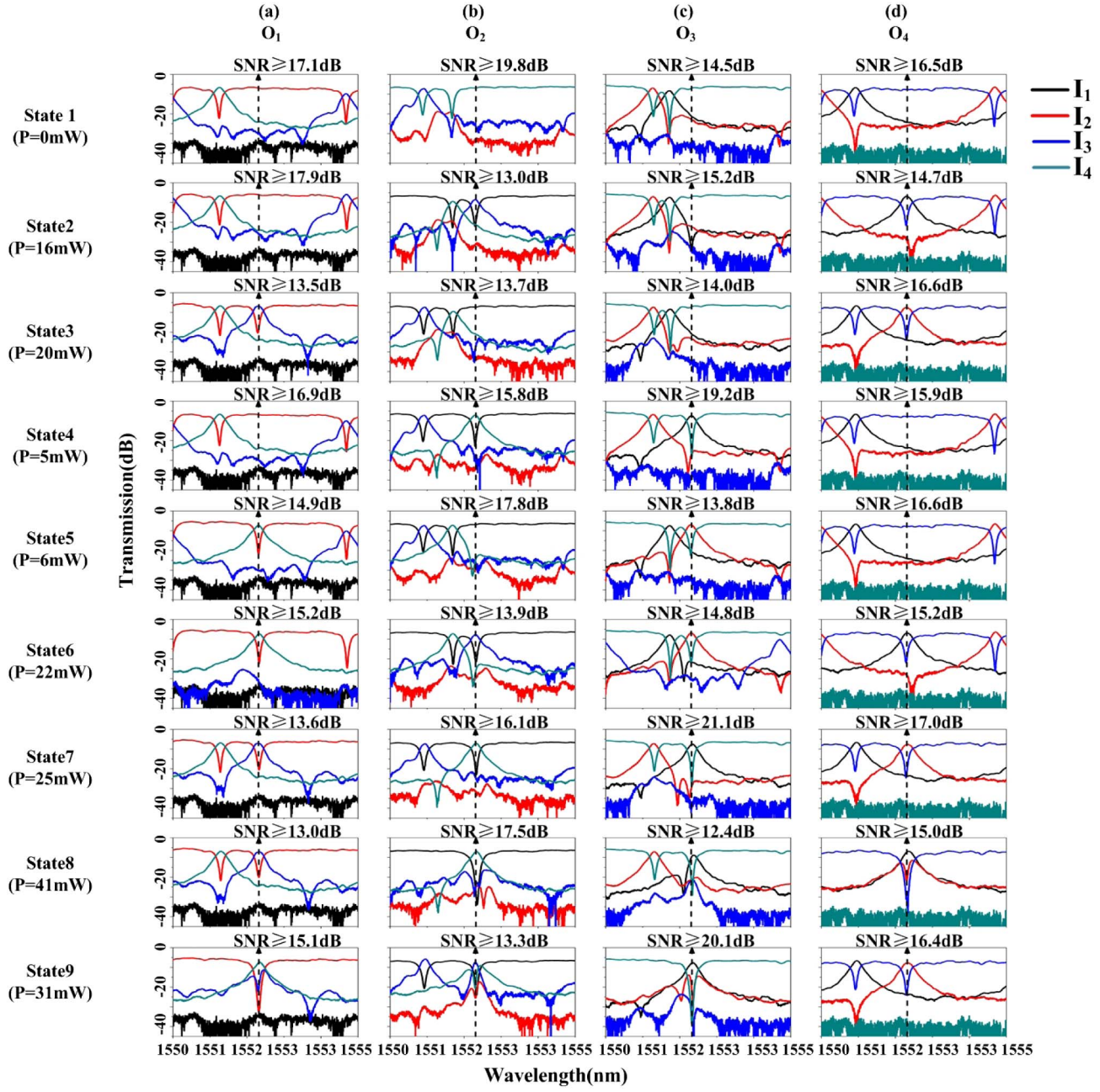

Fig. 4. Optical SNR of the four-port optical router at its nine routing states. Each row shows one routing state, and each column has the same output port. The working wavelength is 1552.31 nm, which is labeled by the dashed line with arrow. Notation P in each row represents total switching power of each routing state.

integrity of 25 Gbps data transmission through the optical router.

As aforementioned, the MR has a periodic spectral response. Therefore, the aggregate bandwidth of the four-port optical router based on MRs can be expanded by WDM technology [18,19]. To verify the property, WDM data transmission is performed for the device. For simplicity, only the results on two representative optical links, $I_1 \rightarrow O_2$ and $I_1 \rightarrow O_3$, which include the "ON" and "OFF" states of the MR optical switches, respectively, are shown in Figs. 6(a) and 6(b). In the wavelength range of 1525–1565 nm, eight optical signals at different wavelengths with the interval equal to FSR can be multiplexed. The clear and open eye diagrams verify the WDM property of the device.

We also create a statistic on the power consumption of the device at the speed of 25 Gbps in its nine routing states. The average energy efficiency is 23 fJ/Bit. As the MRRs are modulated with thermo-optic effect, a 10 KHz square wave is used to manipulate their switching states and measure their response times. The average rising time is 13.3 μs and the average falling time is 12.9 μs.

In conclusion, a reconfigurable non-blocking four-port optical router with the least MR optical switches has been demonstrated. By thermo-optic tuning, the optical SNR of each optical link is characterized. 25 Gbps data transmission has been demonstrated on its whole 12 optical links, and eight-channel WDM data transmission has been implemented to expand its communication capacity. In the future, electro-optic tuning can be

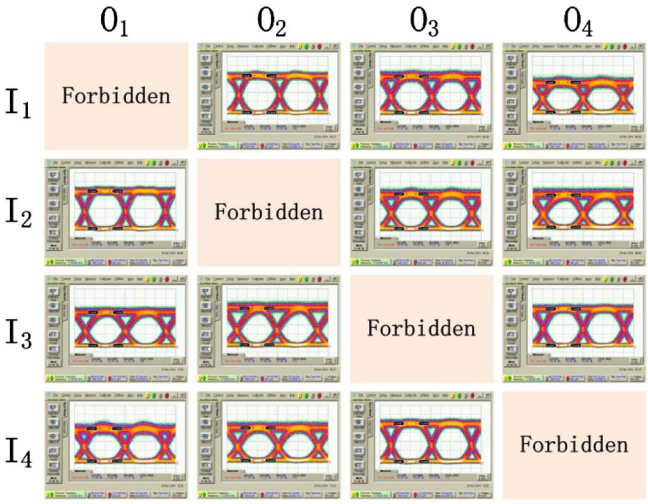

Fig. 5. 25 Gbps eye diagrams for the 12 possible input–output optical links of the four-port non-blocking optical router (data are taken at the working wavelength of 1552.31 nm).

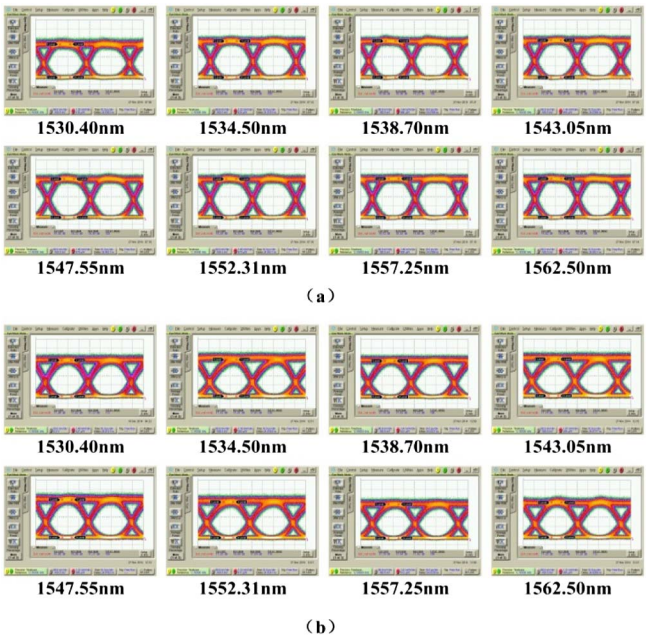

Fig. 6. WDM data transmission through two optical links of the device (a) $I_1 \rightarrow O_2$ and (b) $I_1 \rightarrow O_3$.

adopted to increase its switching speed and decrease its power consumption [15]. Some athermalizing technologies can be adopted to improve the temperature stabilization of the device [20].

The authors thank IME for device fabrication. This work was supported by the National Natural Science Foundation of China (NSFC) under grants 61204061, 61235001, and 61377067, the National High Technology Research and Development Program of China under grants 2015AA010103 and 2015AA010901, and the Scientific and Technological Innovation Cross Team of Chinese Academy of Sciences.

References

1. R. G. Beausoleil, P. J. Kuekes, G. S. Snider, S. Y. Wang, and R. S. Williams, Proc. IEEE **96**, 230 (2008).
2. B. G. Lee, A. Biberman, J. Chan, and K. Bergman, IEEE J. Sel. Top. Quantum Electron. **16**, 6 (2010).
3. A. Joshi, C. Batten, Y. J. Kwon, S. Beamer, I. Shamim, K. Asanovic, and V. Stojanovic, in *Proceedings of the 2009 3rd ACM/IEEE International Symposium on Networks-on-Chip* (IEEE, 2009), pp. 124–133.
4. D. A. B. Miller, Proc. IEEE **97**, 1166 (2009).
5. H. X. Gu, K. H. Mo, J. Xu, and W. Zhang, in *2009 IEEE Computer Society Annual Symposium on VLSI* (IEEE, 2009), pp. 19–24
6. A. W. Poon, X. S. Luo, F. Xu, and H. Chen, Proc. IEEE **97**, 1216 (2009).
7. T. Hu, H. Qiu, P. Yu, C. Qiu, W. Wang, X. Jiang, M. Yang, and J. Yang, Opt. Lett. **36**, 4710 (2011).
8. R. Q. Ji, L. Yang, L. Zhang, Y. H. Tian, J. F. Ding, H. T. Chen, Y. Y. Lu, P. Zhou, and W. W. Zhu, Opt. Express **19**, 20258 (2011).
9. N. Sherwood-Droz, H. Wang, L. Chen, B. G. Lee, A. Biberman, K. Bergman, and M. Lipson, Opt. Express **16**, 15915 (2008).
10. A. Kazmierczak, W. Bogaerts, E. Drouard, F. Dortu, P. Rojo-Romeo, F. Gaffiot, D. Van Thourhout, and D. Giannone, IEEE J. Lightwave Technol. **27**, 3317 (2009).
11. R. Q. Ji, L. Yang, L. Zhang, Y. H. Tian, J. F. Ding, H. T. Chen, Y. Y. Lu, P. Zhou, and W. W. Zhu, Opt. Express **19**, 18945 (2011).
12. Y. Y. Ye, X. W. Wu, J. Xu, W. Zhang, M. Nikdast, and X. Wang, in *IEEE International Conference on Anti-Counterfeiting, Security and Identification (ASID)* (IEEE, 2012), pp. 1–5.
13. R. Min, R. Q. Ji, Q. S. Chen, L. Zhang, and L. Yang, IEEE J. Lightwave Technol. **30**, 3736 (2012).
14. Q. Chen, F. F. Zhang, R. Q. Ji, L. Zhang, and L. Yang, Opt. Express **22**, 12614 (2014).
15. M. Yang, W. M. J. Green, S. Assefa, J. Van Campenhout, B. G. Lee, C. V. Jahnes, F. E. Doany, C. L. Schow, J. A. Kash, and Y. A. Vlasov, Opt. Express **19**, 47 (2011).
16. M. S. Dahlem, C. W. Holzwarth, A. Khilo, F. X. Kärtner, H. I. Smith, and E. P. Ippen, Opt. Express **19**, 306 (2011).
17. X. S. Luo, J. F. Song, S. Q. Feng, A. W. Poon, L. T. Yang, M. B. Yu, G. Q. Luo, and D. L. Kwong, IEEE Photon. Technol. Lett. **24**, 821 (2012).
18. A. Biberman, B. G. Lee, N. Sherwood-Droz, M. Lipson, and K. Bergman, IEEE Photon. Technol. Lett. **22**, 926 (2010).
19. R. Q. Ji, J. Xu, and L. Yang, IEEE Photon. Technol. Lett. **25**, 492 (2013).
20. K. Padmaraju and K. Bergman, Nanophotonics **3**, 269 (2014).